JOURNAL OF GEOPHYSICAL RESEARCH, VOL. 104, NO. C8, PAGES 18,111-18,126, AUGUST 15, 1999

Cyclogenesis in the deep ocean beneath the Gulf Stream 1. Description

Dana K. Savidge and John M. Bane Jr.

Department of Marine Sciences, University of North Carolina, Chapel Hill

Abstract. One of the primary scientific results of the Synoptic Ocean Prediction (SYNOP) observational program was the discovery of strong cyclones in the deep ocean beneath the large amplitude Gulf Stream meander troughs that routinely form at about 68°W. These strong well-organized cyclones extend to at least 3500 m below the sea surface and are an important component of the overall dynamical variability of the Gulf Stream and adjacent deep waters. Typically, a small amplitude Gulf Stream meander "stalls" near 68°W and begins to amplify. As the amplitude of troughs in the Gulf Stream jet increases, the currents at 3500 m strengthen and turn, forming a cyclonic circulation pattern. During SYNOP, six well-defined instances of meander trough amplification and deep cyclogenesis occurred. The cyclones were characterized by strong swirl speeds (up to 0.5 m s^{-1}) and were long-lived (typically lasting 6-9 weeks) frequent occurrences (present 35% of the time during the 25 month deployment period). The structure of the cyclones at 3500 m is characterized by increasing velocity from the cyclone center out to some radius of maximum velocity and decreasing velocity beyond that radius. This structure was robust over the lifetime of an event and from event to event. Cyclone radius and the radius to maximum velocity were consistently $\simeq$ 130 km and $\simeq$ 55 km, respectively. Evidence of cyclones at upper measurement levels and the low vertical shear values apparent in the deep water below the thermocline indicate that the cyclones extended throughout the entire water column; from the benthic boundary layer, through the thermocline, and to the ocean's surface.

1. Introduction

The Synoptic Ocean Prediction (SYNOP) Experiment's observational program provided unprecedented spatial and temporal coverage of the Gulf Stream and its surrounding environment downstream from Cape Hatteras [*Johns et al.*, 1995; *Shay et al.*, 1995; *Watts et al.*, 1995; *Bower and Hogg*, 1996]. One of the primary scientific results of the program was the discovery of strong, transient cyclones in the deep ocean beneath the large amplitude Gulf Stream meander troughs that routinely form in the Gulf Stream's path. Several such events were directly observed at about 68°W, the location of the SYNOP Central Array (Figure 1). While strong velocities in the deep ocean near this location had been observed before [*Luyten*, 1977; *Hogg*, 1981], it was not until SYNOP that these flows were clearly seen to be part of well-organized mesoscale cyclones, strongly coupled to the evolution of the Gulf Stream path in the upper ocean. The cyclones observed in the SYNOP Central Array at 3500 m were characterized by strong swirl speeds (up to 0.5 m s^{-1}) and were long-lived (typically lasting 6-9 weeks) frequent occurrences (present 35% of the time during the 26 month deployment period). The strong cyclonic flows extended throughout essentially the entire water column, from the benthic boundary layer up into and above the thermocline. The purpose of this paper is to describe these cyclones. Naturally, the processes responsible for their generation are also of interest. The dynamics of deep ocean cyclogenesis have been examined and are described by *Savidge and Bane* [this issue]. The emphasis in these two papers is on the structure and evolution of flow in the deep ocean. The intimately related topic of Gulf Stream path evolution in the upper ocean has been addressed by *Howden* [1996].

During the tenure of the SYNOP Central Array moorings (data used in this study are from June 13, 1988, to August 7, 1990), six well defined instances of meander trough amplification and deep cyclogenesis occurred. A time series of horizontal maps of data from the Central Array during one episode illustrates the typical scenario (Figure 2). On May 5, 1990, there was a small amplitude meander trough entering the Central Array from the west. Large amplitude meander crests and ring-Stream interactions immediately downstream are apparent in satellite sea surface temperature (SST) imagery prior to or during this and all five other deep cyclogenesis events during SYNOP (Figure 3). The trough amplified into a large, southward looping meander over the following two weeks. During this time, currents at the 3500 m level evolved from weak, generally westward flow to strong cyclonic flow, with velocities in excess of 0.25 m s^{-1} at many locations. The perturbation pressure field at 3500 m

Paper number 1999JC900132.
0148-0227/99/1999JC900132$09.00

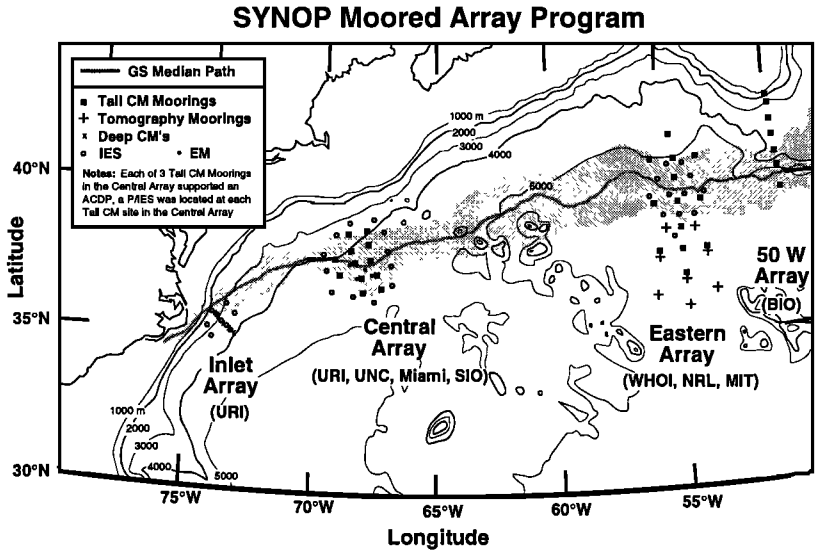

Figure 1. Map of the northwestern North Atlantic showing the SYNOP mooring arrays. The bold line indicates the median location of the northern edge of the Gulf Stream during the experiment. The shading represents the envelope within which the Gulf Stream path was located during the experiment. The path was located south of the light shaded region only 1% of the time, south of the dark shaded region 10% of the time, north of the dark shaded region 10% of the time, and north of the light shaded region 1% of the time.

developed an intense low pressure center downstream from the Gulf Stream trough axis. The perturbation exceeded 3.5×10^3 Pa (-0.35 dbar) at the cyclone center on May 25. Cyclones disappeared as the meander trough amplitude decreased, moved downstream, or pinched off to form a cold-core ring. Then the deep cyclonic flow slowed and became less organized or drifted out of the Central Array. Though one month of data is illustrated in Figure 2, this particular event lasted almost nine weeks.

Such strong organized flow in the deep ocean beneath the Gulf Stream is perhaps unexpected but should not be based on analogy with the atmospheric jet stream. In the atmosphere, the generation of surface low and high pressure systems is intimately associated with the evolution of jet stream waves, through the process of baroclinic instability [*Palmen and Newton*, 1969]. In fact, strong flows have been seen earlier in the deep ocean. Such observations include those near 73°W [*Johns and Watts*, 1986], those in the Rise Array at a location immediately upstream the SYNOP Central Array location [*Luyten*, 1977; *Hogg*, 1981], those from the HEBBLE experiment site at 62°W [*Kelley et al.*, 1982], and those from the POLYMODE experiment and the Gulf Stream Array downstream from the New England Seamounts near 55°W [*Hendry*, 1982]. In several of these cases, the strong flows have been hypothesized to be topographic Rossby waves, which are a different phenomenon than the deep cyclones. However, these observations also include instances of strong deep flow that do not resemble topographic Rossby waves. These observations may reflect features in the flow that are similar to the deep cyclones at 68°W but were observed with insufficient spatial coverage to resolve the complete flow pattern. Interestingly, a likely source for topographic Rossby waves observed just northeast of Cape Hatteras has been suggested to be Gulf Stream Ring formation or meanders [*Hogg*, 1981; *Csanady*, 1982]. Efforts to find the source region have led to the area where the observed SYNOP deep cyclones occur [*Hogg*, 1981; *Pickart*, 1995].

The effect of the SYNOP Central Array cyclones on the mean flow there is illustrated in the record-long average currents, which show cyclonic flow at 3500 m depth (Figure 4, left) [*Shay et al.*, 1995]. If the 3500 m velocity data from this period are split into event days and nonevent days (event specification is discussed in section 3) and averages computed for each data subset, it becomes clear that the record-long mean cyclonicity at 3500 m was a result of the deep cyclone events described above. During cyclone events, average currents were generally southwestward in the northern half of the array and were strong and cyclonic in the southern half (Figure 4, middle). In the absence of deep cyclones, the average currents at 3500 m show generally southwestward flow in the northern half of the array and weak unorganized flow in the southern half (Figure 4, right). Standard errors (ϵ) are plotted as boxes at the vector tips and were calculated as $\epsilon = \left(\sigma^2/(n/\tau)\right)^{\frac{1}{2}}$, where σ^2 is the time series variance, n is the length of the series in days, and τ is the decorrelation timescale, here 5.4 days for the u time series and 4.9 days for the v time series, as calculated by *Shay et al.* [1995].

The recurring meander troughs near 68°W, with which the deep cyclones are associated, affect the mean Gulf Stream path as well. *Lee and Cornillon* [1996] show a slight trough in the mean Gulf Stream path at approximately 68°W, calculated from 7 years of satellite sea surface temperature data. A slight trough is also seen in the median Gulf Stream lo-

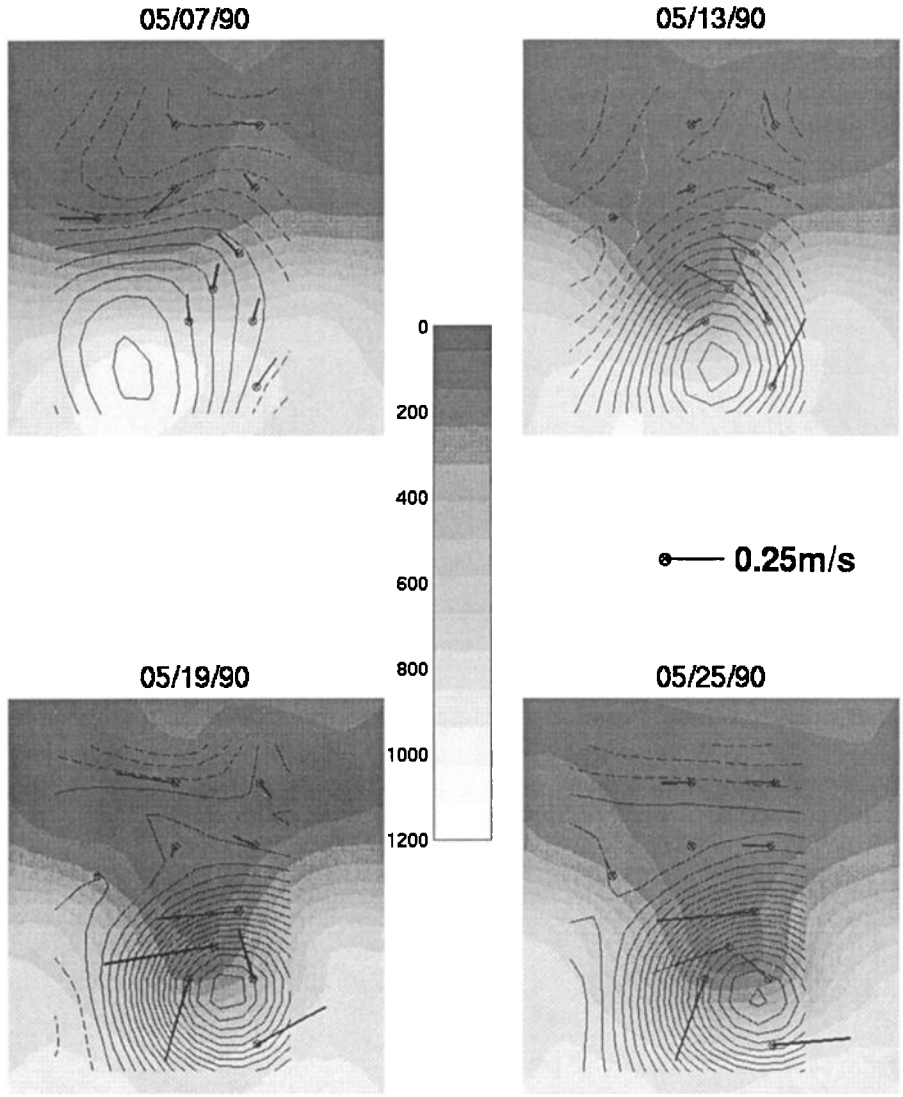

Figure 2. Time series of horizontal maps of data from the SYNOP Central Array at 6 day intervals, over an approximately 300 by 300 km area. These maps show the development of a steep meander trough in the Gulf Stream and a strong cyclone at 3500 m. The gray scale field represents the depth of the 12°C isotherm. The Gulf Stream jet closely follows the portion of the thermocline that slopes steeply from 200 to 800 m depth in the middle 1/3 of the array. The 13 current meter moorings of the Central Array are shown as circles with crosses. Vectors represent measured velocities at 3500 m. The contoured field is the optimally interpolated perturbation pressure field at 3500 m. Contour interval is 2×10^2 Pa (0.02 dbar); solid lines indicate negative values.

cation during the SYNOP experiment (Figure 1). Additionally, the limited area North Atlantic model of *Thompson and Schmitz* [1989] shows that once the model reaches equilibrium, a large Gulf Stream meander trough exists in the vicinity of 37°N, 68°W, accompanied by mean cyclonic circulation in the deep layer, consistent with the SYNOP Central Array observational data.

2. Data and Data Products

The data used here were acquired as part of the SYNOP experiment. The observational component of SYNOP included four instrument mooring arrays along the Gulf Stream mean path downstream of Cape Hatteras, several hydrographic cruises, isopycnal RAFOS float deployment, and the acquisition of satellite measurements of sea surface temperature. This study uses data from the Central Array, which was located over an approximately 300 km by 300 km area centered at 37.5°N, 67.5°W(Figure 1). This array consisted of 12 tall current meter (CM) moorings with horizontal velocity, temperature (T), and pressure (p) sensors at target depths of 400, 700, and 1000 m, and horizontal velocity and T sensors at 3500 m. Bottom pressure sensor and inverted echo sounder (IES) moorings were colocated with the 12 CM moorings. An additional ring of 13 bottom mounted IES moorings encircled the 12 central CM/P/IES moorings (Figure 3). The complete array was in place from May 1988 through August 1990, a period in excess of two years. A

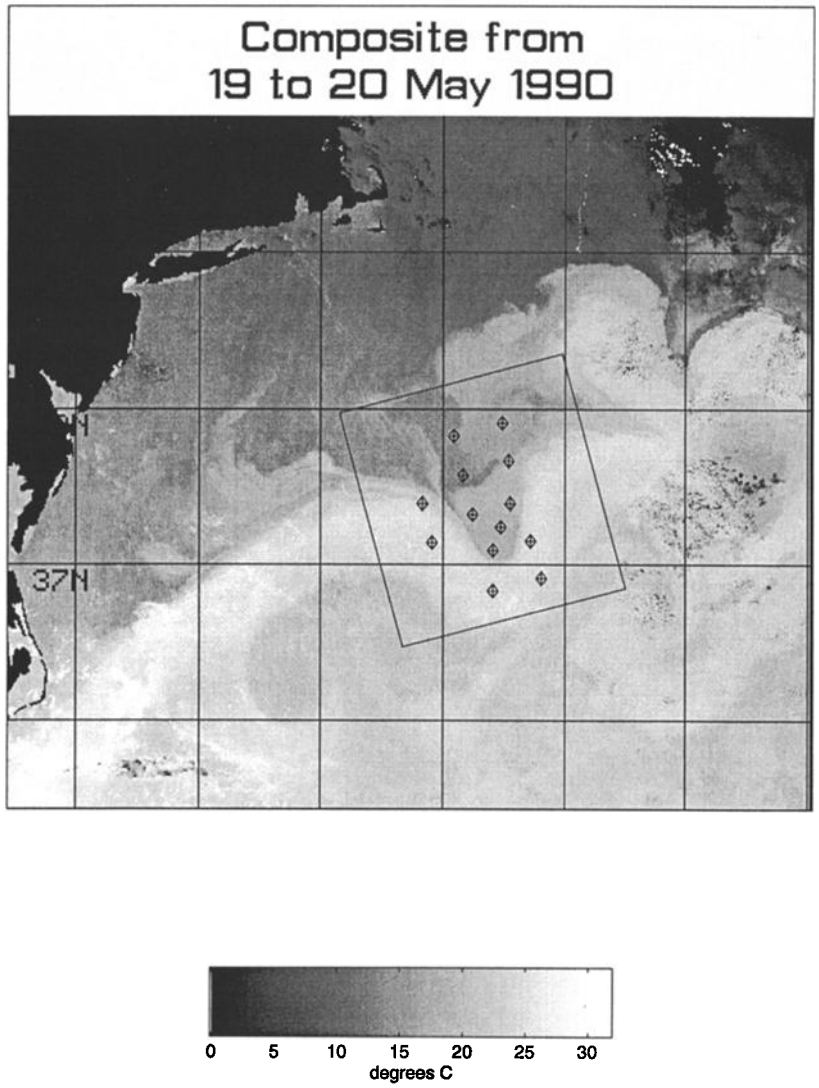

Figure 3. Composite image of satellite advanced very high resolution radiometer sea surface temperature for May 19-20, 1990. The image shows an example of a steep meander trough in the SYNOP Central Array. Also shown are the locations of the tall current meter moorings in the Central Array (diamonds with crosses) and the area (box) over which the depth of the 12°C isotherm can be optimally interpolated from the inverted echo sounders deployed in the Central Array. This box is the same area covered by Figures 2, 4, 6, and 13. (Image prepared by the P. Cornillon group of Univ. of Rhode Island.)

13th CM mooring was deployed during the second half of the experiment.

Current, temperature, and pressure data from the EG&G Vector averaging current meters (VACMs) and Aanderaa current meters (AACM) on the tall current meter moorings were processed as follows. Velocities were decomposed into u and v components in a right-hand Cartesian coordinate system whose x axis was 15° counterclockwise from due east, such that the u component was pointed in the mean downstream direction of the Gulf Stream jet at 400 m in this location. The u,v, and T data were filtered using a 40 hour low-pass (40HLP) Butterworth filter and subsampled. The current and temperature data from the upper three levels were then corrected for mooring motion using the scheme of *Hogg* [1991], modified for SYNOP data by *Cronin and Watts* [1996]. More complete descriptions of the processing are given by *Watts et al.* [1995] and *Shay et al.* [1995]. Bottom pressures recorded at the CM locations were corrected to a common level (3500 m) using the method of *Qian and Watts* [1992] and *Watts et al.* [1995]. These pressures were filtered with a 40HLP Butterworth filter and subsampled. Velocities and temperatures from all four measurement levels and bottom pressures corrected to 3500 m depths were also optimally interpolated (OI) to uniform grids by the D. R. Watts group of the University of Rhode Island (URI), and those maps are utilized here. Details of that processing are given by *Cronin* [1993] and *Qian and Watts* [1992]. A two-pass OI method was used to precondition the fields, such that the OI requirement for isotropic homogeneous fields was not violated. Briefly, the fields were optimally interpolated once

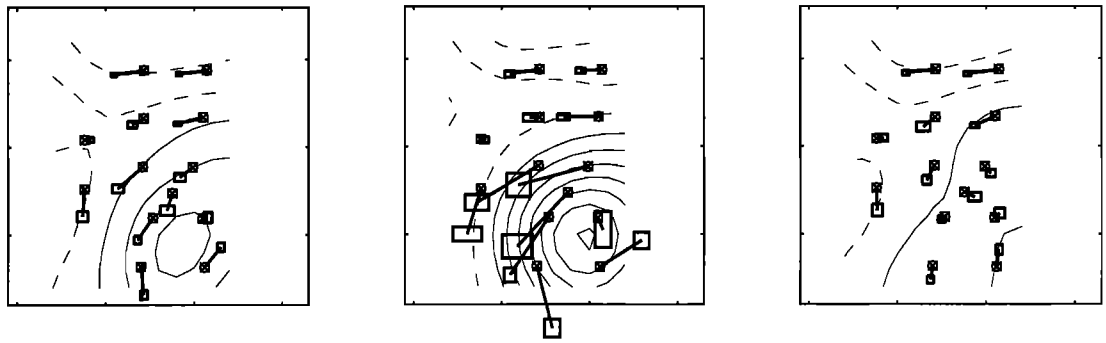

Figure 4. Mean measured velocities with standard errors and optimally interpolated perturbation pressure fields at 3500 m in the SYNOP Central Array. (left) Record long means, (middle) means over cyclone event days only, and (right) means over all days in record except cyclone event days. Pressure field contour interval is 2×10^2 Pa (0.02 dbar); solid lines indicate negative values.

using a large correlation length, and means and standard deviations were calculated at locations of input data and desired output. That information was then used to demean and normalize the input data and to restore appropriate means and variances to the output fields, which were calculated the second time with a reduced correlation length.

Inverted Echo Sounders were deployed at 25 locations in the SYNOP Central Array to measure the depth of the 12°C isotherm (Z12 depth). Using the methods of *Tracey and Watts* [1991], the data were optimally interpolated to a uniform grid. The resultant maps were used here primarily to locate the Gulf Stream in the Central Array, since according to *Kim and Watts* [1994], they can be used as a stream function for the Gulf Stream. Locations of the strongest slope in the Z12 surface correspond to the horizontal locations of fastest near-surface jet velocities. The depth of the 6°C isotherm (Z6 depth) was calculated from the Z12 maps according to $Z6 = Z12a + b + Kc$, at the suggestion of D. R. Watts. That is, Z6 was calculated as a linear function of Z12 plus a small correction for Gulf Stream curvature (K) (the steepness of the thermocline changes with curvature). Here the constants $a = 1.05$, $b = 270$, and $c = 500$ were calculated as a best fit to accumulated historical data in this location by K. Tracey. Gulf Stream curvature was calculated from Z12 fields according to a method devised by Xiaoshu Qian. Briefly, this method utilizes two-dimensional ("2-D") tensor product spline fits (fit is calculated first in one direction then in the second) of the optimally interpolated Z12 fields, minimizing the weighted average of mean square error and the integrated (in space) second derivative. This 2-D analytical function can then be used to calculate curvature based on the formula for the intersection of a surface and a plane, which can be found in standard analytical geometry textbooks:

$$K = \frac{Z_x{}^2 Z_{yy} + Z_y{}^2 Z_{xx} - Z_x Z_y \left(Z_{xy} + Z_{yx}\right)}{\left(Z_x{}^2 + Z_y{}^2\right)^{\frac{3}{2}}}.$$

Here the Z values represent the analytical Z12 surface, and the subscripts x and y represent spatial differentiation in two horizontal directions.

Satellite advanced very high resolution radiometer sea surface temperature maps were utilized here to ascertain Gulf Stream position on days of low cloudiness. These data were processed by the P. Cornillon group of URI.

Measured temperatures at the four measurement levels were converted to densities by first calculating salinities (S) from T according to the algorithm of *Armi and Bray* [1982]. This was done iteratively, since the *Armi and Bray* [1982] algorithm requires potential temperature (θ), which requires knowledge of S. Using in situ T as a first guess for θ, S was calculated, then used to calculate θ from T, which was then used to recalculate S. This was done until the change in S from step to step fell below 0.0001 practical salinity unit (psu). This small value is below the accuracy of the *Armi and Bray* [1982] algorithm by an order of magnitude. For representative values of T and p at the measurement levels, this error in S amounts to approximately an error of 0.001 kg m^{-3} in density. The estimated S, the in situ T, and the appropriate p were then used to calculate density at the mooring locations and on a uniform grid. Horizontal gradients in density were calculated using OI (see *Bretherton et al.* [1976] for discussion of the use of OI to calculate derivatives of measured quantities). The OI derivatives agree well with estimates of the gradients made using finite difference approximations. The advantage of the OI approach over the finite difference approach is that estimates can be made at a wider variety of locations.

3. Specification of Cyclone Events

Periods of deep cyclone events are characterized by (1) large Gulf Stream curvature, (2) higher than average current speed at 3500 m, and (3) the persistence of strong cyclonic organized flow for an extended period of time (events typically last 6-9 weeks). These three features were used to identify deep cyclone events in the SYNOP Central Array data set: First, a threshold Gulf Stream curvature value was defined as ± 0.0125 km^{-1}, above which a cyclone at 3500 m was considered possible. Data were sorted into "straight" Gulf Stream and "curved" Gulf Stream bins on this basis. The specification of events is robust to the threshold value

chosen [*Savidge*, 1997]. An average background current speed at 3500 m of 0.096 m s^{-1} was then calculated from the straight Gulf Stream data, over all moorings and all days in that bin. The event day list was then refined by comparing the daily domain wide average velocities at 3500 m to this background. When the daily averages exceeded the background for more than a few days, the flow field at 3500 m was inspected, and cyclonic events were identified. On this basis, six clear instances of cyclogenesis were defined and specified by letter names A-F (Figure 5). These events included 275 days out of a total 786 in the data set used here, constituting 35% of the time. Several other strong flow events at 3500 m were also identified via the event criteria. These events were anticyclonic or straight flow and were less energetic and less organized than the cyclone events. They have not been closely examined here. These episodes included 166 days, constituting an additional 21% of the time.

The cyclonic events showed some strong similarities to each other, as described in the following sections. However, there was some variability among the events. Events C and F were characterized by the strongest velocities of the six events and were the most long-lived. Event A was also fairly strong, with events B, D, and E trailing it in strength. Two of the events, D and E, were not considered extensively in the following analysis. Event D started one day after event C ended and was followed by an extended period of time during which the Gulf Stream path was quite convoluted and flow at 3500 m was particularly energetic and complex (the "S-meander" phase described by *Shay et al.* [1995]). The start and stop days of event D were consequently slightly more arbitrary than the other events, and the generally high energetic level of the time period in which it was imbedded makes its salient features more difficult to determine. The cyclone at 3500 m during event E was located slightly farther downstream than the other events and so was less well resolved by the Central Array instrumentation than the other events. The apparent location of this cyclone's center was eastward of the easternmost mooring throughout the event. The demise of the cyclones also showed some variability. Event A ended as a cold-core ring pinched off from the Gulf Stream trough that had formed in association with the deep cyclone; events B and E ended with trough and cyclone both relaxing and drifting downstream; events C and D ended as their associated troughs diminished in amplitude and were followed immediately by periods of complex Gulf Stream path geometry.

4. Movement of the Cyclones

The cyclonic features seen in the deep flow fields were not rigidly fixed in one position throughout the events but moved in space and in relation to the Gulf Stream jet structure. The location of a low pressure center in the perturbation pressure field at 3500 m was taken as the "center" of a deep cyclone. These locations were selected manually at daily intervals by inspection of the contoured 3500 m optimally interpolated pressure maps. Strickly speaking, error resulting from this manual process is at least the spacing between grid points, 20 km (the distance chosen by the D. R. Watts group as the optimum spacing for their OI fields). However, every effort was made to select the location of the low pressure centers indicated by the contouring routine to within a smaller distance than that; to 10 km or less in either the x or y direction. Spot checks of the pressure at those locations using OI indicates that the contouring program's low pressure center locations were indeed characterized by pressure lower than found at the grid points. This suggests that the actual error may be less than the 20 km grid point spacing. Once the centers were chosen, it was possible to calculate a variety of descriptive measures following each cyclone. These measures included the path of a cyclone relative to topography, the pressure value at the center through time, the pressure gradient resulting from the decreasing pressures at cyclone center, the average speed of the current about the center, the depth of the subthermocline water layer at the cyclone center, and the position of the cyclone center relative to the Gulf Stream meander trough axis. These measures are discussed in the following paragraphs.

The paths of the low pressure centers illustrate a difference between the strongest events, C and F, and the other events (Figure 6). For these two events, the low pressure centers started near the 4250 m isobath in the western central

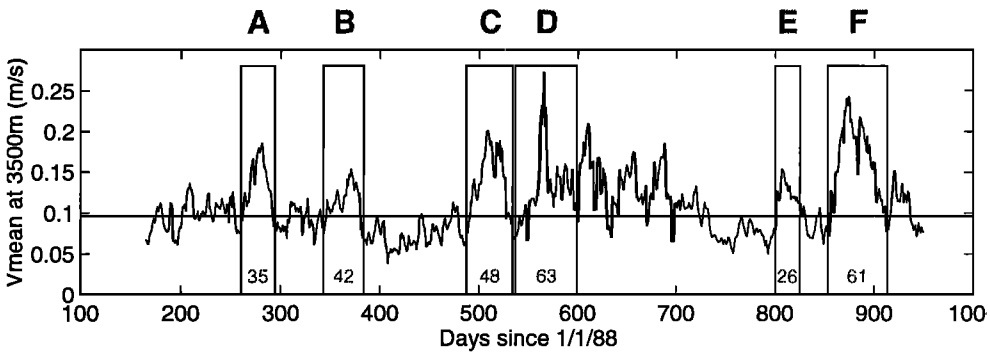

Figure 5. Time series of daily domain-wide average current speed at 3500 m. The horizontal line is the "background" velocity at 3500 m, calculated as defined in the text. Cyclone events are boxed and labeled with letter designations and the number of days in each event. Extended periods of strong flow that are not boxed and labeled are periods of anticyclonic, straight, or unorganized strong flow at 3500 m.

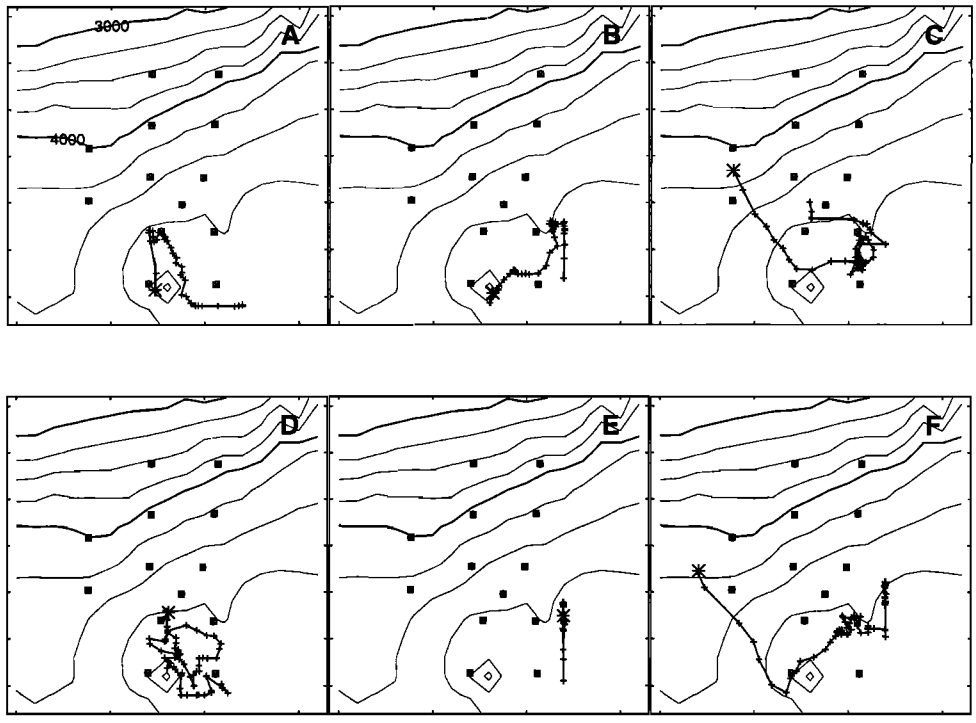

Figure 6. Paths of cyclones (low pressure centers at 3500 m) and bottom topography for events A through E. Starting locations are indicated (asterisks), as are daily noon locations (crosses). On days when the cyclone centers were located eastward of the array, the centers were taken as the location of the lowest pressure along the eastern edge of the region over which the pressure field was optimally interpolated. This resulted in the apparent (but fictional) straight line north-south motion of the cyclones seen here.

part of the array, then moved rapidly southeastward across topography to approximately the 4750 m isobath, covering a distance of $\simeq$ 150 km in 6-7 days. The cyclones then turned to the N-NE, passed to the N-NW of Caryn Seamount, and crossed the deepest topography (deeper than 4800 m) to the N-NE of that seamount before ceasing to intensify. The weaker cyclones were characterized by centers that started their lives near Caryn Seamount, in water about 4600 m deep. They then moved about in the region of deep water near Caryn Seamount and intensified (Figure 6).

The pressure anomaly at each low pressure center was calculated by linear interpolation of the OI pressure fields (Figure 7, left) (except event E, see section 3). Each low intensified through the first few weeks of its lifetime. During this intensification, the magnitude of the average horizontal pressure gradient near the radius of maximum velocity increased (Figure 7, right), as did the domain-wide velocity average (Figure 5). The average pressure gradient near the radius of maximum velocity was calculated from finite difference estimates calculated from the OI pressure fields, converted to magnitudes, and averaged over locations between 30 and 100 km from the cyclone centers. These limiting radii were chosen in order to average over the region of largest velocities associated with the low pressure centers (see section 5). Events C and F reached much lower pressure and higher pressure gradient magnitudes than the other events, and their initial rates of pressure change were also greater.

The thickness of the lower layer following the cyclone center was also calculated. Here the lower layer was defined as the water between the 6°C isothermal surface and the ocean bottom. Total ocean bottom depths following the cyclone centers were also determined and are shown in Figure 8, left. Events A, B, C, and F show gradual thickening of the lower layer of $\simeq$ 900 km over the first 25 event days, consistent with pressure values at the low pressure centers, which showed a rather linear decrease over the first 20-30 days of all events. Taking 3500 m as the typical starting thickness (from the plots), this amounts to a $\simeq$ 25% increase in layer thickness. If potential vorticity is conserved ($D(f+\zeta)/H = 0$), this suggests the development of considerable relative vorticity, of $O(0.25f)$, assuming (1) planetary vorticity (f) varies little along the cyclone center's path and (2) negligible relative vorticity to start. This is consistent with the calculations of cyclone relative vorticity made in section 5, which approach $0.2f$ at the cyclone center. The lack of significant stretching in event D is puzzling.

These calculations do not suggest the stretching occurred as a result of the motion of the cyclone centers over deepening bathymetry. The lower layer thickness of the two strongest events C and F did not show a significant increase at cyclone center during the first 6-7 days of rapid travel over deepening bathymetry (Figure 8). The depth of the lower layer columns were also strongly controlled by their placement with respect to the Gulf Stream jet axis and by

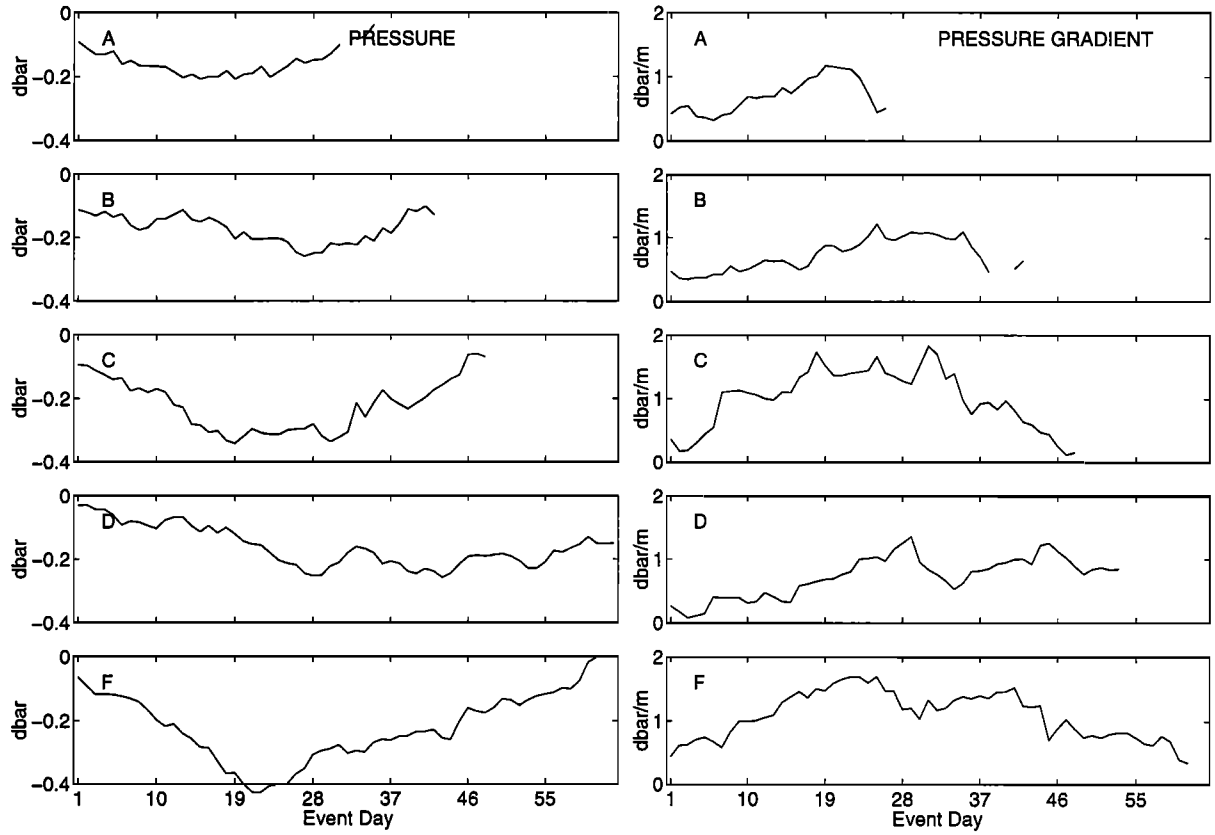

Figure 7. Time series of selected quantities following cyclone center: (left) pressure at cyclone centers (10^4 Pa or 1 dbar), and (right) average pressure gradient at radii between 30 and 100 km (10^{-2} Pa m^{-1} or 10^{-6} dbar m^{-1}).

the deepening of the thermocline in the offshore direction associated with the jet, as can be seen in the difference between the bottom depth and the lower layer thickness (Figure 8) following cyclone centers. *Savidge and Bane* [this issue] show that the stretching resulted from strong vertical velocities in the main thermocline, resulting mainly from flow along the strongly sloping permanent thermocline.

Cyclogenesis due to baroclinic instability requires a downstream offset between the upper layer jet stream trough axis and the center of the lower layer cyclone. The demise of cyclones is associated with a decrease in the offset and a corresponding decrease in energy conversion through baroclinic instability [*Holton*, 1979]. Estimates of the trough axis/cyclone center offsets in the oceanic cases here were made by extending a perpendicular line horizontally from the cyclone center to a line designating the location of the upper level trough axis. This line was established manually on daily horizontal maps of curvature of the Z12 surface, calculated as described in section 2. The error in location of the lines was large, perhaps up to 20 or 30 km, especially during early days of cyclone events when the curvature in the troughs was slight and fairly uniform, and in the later days if Gulf Stream structure became complex. However, the estimated offsets suggest that the low pressure centers were generally located downstream from the trough axes and that the offsets decreased gradually over the cyclone lifetimes (Figure 9). The maximum offset seems to be about 50 km, or 1/6th of a 300 km wavelength. Typical values are not inconsistent with those reported by *Watts et al.* [1995] of approximately 1/16th to 1/8th of a wavelength.

5. Horizontal Velocity Structure

The horizontal velocity structure of the SYNOP cyclones at 3500 m was assessed using both the measured and OI velocities. In both cases, the horizontal velocity was converted to azimuthal and radial velocities ($u_{swirl} = rd\theta/dt$, $u_r = dr/dt$ where θ and r are azimuthal and radial positions) about an origin taken to be the cyclone center location on a given day. Positive u_{swirl} and u_r are defined as counterclockwise motion and motion away from cyclone center, respectively. Scatter plots of OI u_{swirl} and u_r versus radius for event F show essentially circular flow, as seen by the small magnitudes of u_r values calculated, relative to the magnitudes of u_{swirl} (Figures 10, top and 10, middle). Swirl velocities increased with radius out to a radius of maximum velocity (about 55 km) and decreased beyond that radius (Figure 10, top) . The measured velocities show a consistent picture (Figure 10, bottom) but provide less spatial coverage than the OI velocities. Results from other events (not shown) verify the radial structure seen in the OI velocity scatter plots at essentially all radii. The secondary maximum seen at large radii results from the westward flow at the northern end of the Central Array. Westward flow typically

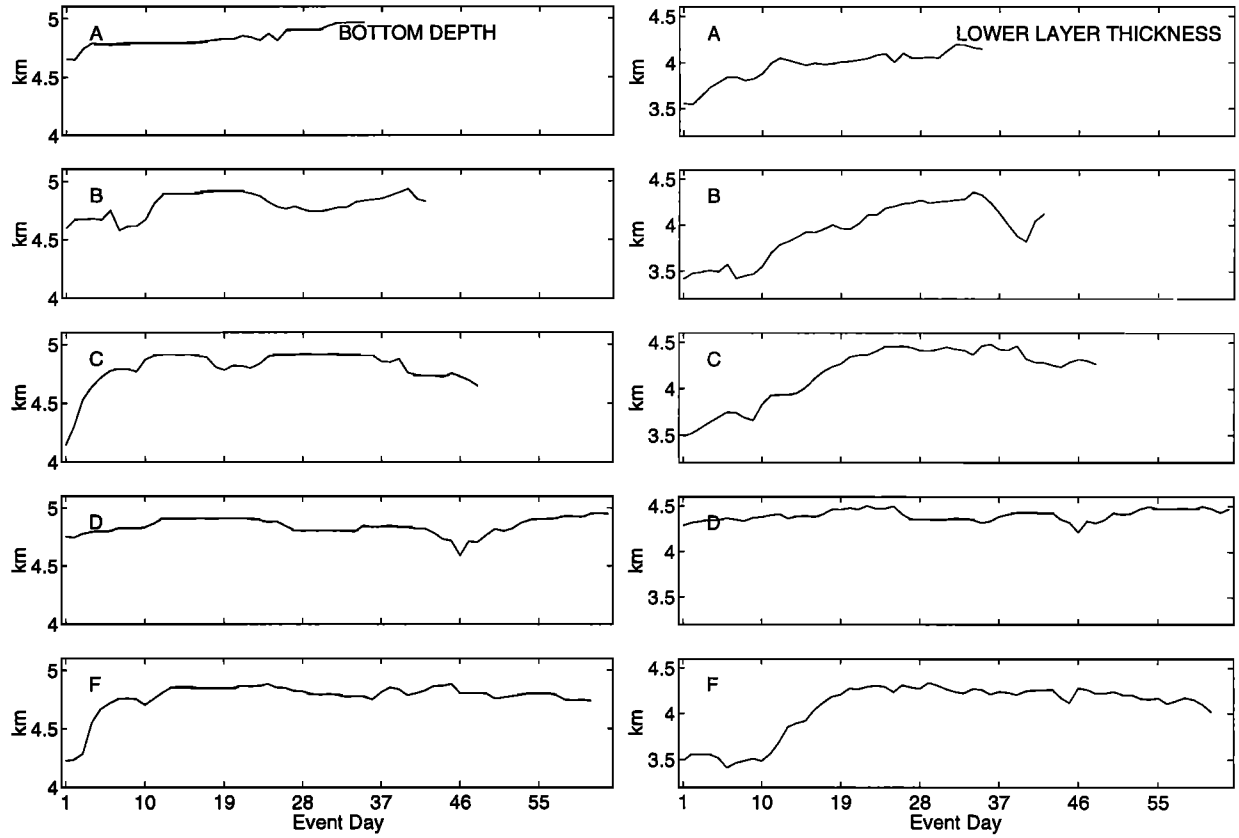

Figure 8. Time series of selected quantities following cyclone center: (left) bottom depth and (right) depth of the water column between the bottom and the 6°C isotherm at cyclone center locations (lower layer thickness).

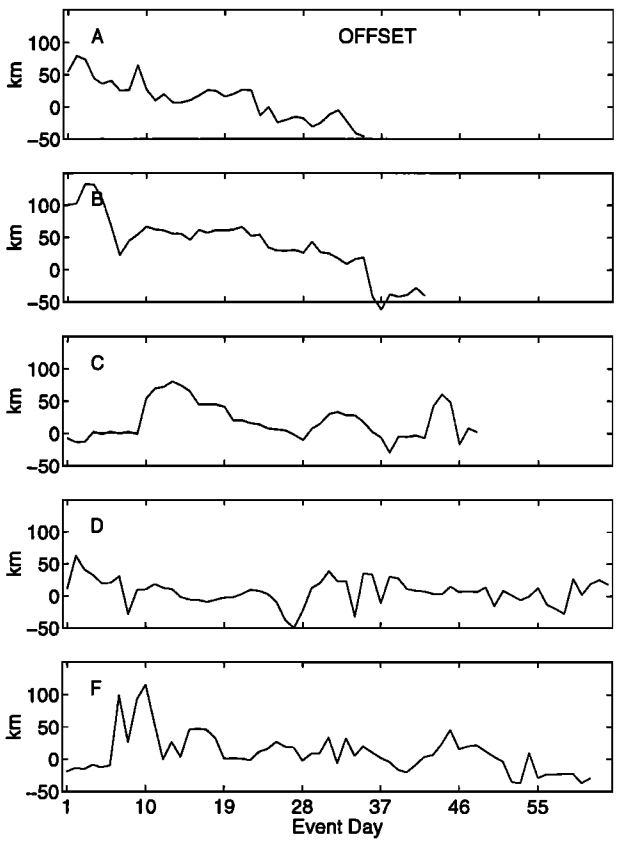

Figure 9. Downstream offset between the Gulf Stream trough axis and the low pressure centers at 3500 m, calculated as discussed in the text. Positive values indicate low pressures were downstream from trough axis.

appears at the northernmost moorings during cyclone events as well as during nonevent times (Figure 4), and it is postulated to be Deep Western Boundary Current flow [*Shay et al.*, 1995]. It appears at large radii in this sorting since the cyclones spend most of their lifetimes centered in the southeast corner of the Central Array (Figure 6). The largest OI u_{swirl} values result not from large Deep Western Boundary Current flow measured at the northernmost mooring but from the extrapolation of those velocities and weaker velocities to their south to the northern edge of the OI domain.

The data were binned according to radius to calculate average velocity as a function of radius. Averages over "developing" days of a cyclone and "fully developed" days were calculated for each event (except event E, see section 3), over all days of each event, and for days of all events pooled (Figure 11). Developing days were defined as days from the start of an event up to and including the day of maximum domain-wide average velocity at 3500 m, and fully developed days were defined as all event days thereafter. Two significant points are evident here. First, the radial structure and cyclone size did not change dramatically over the lifetime of

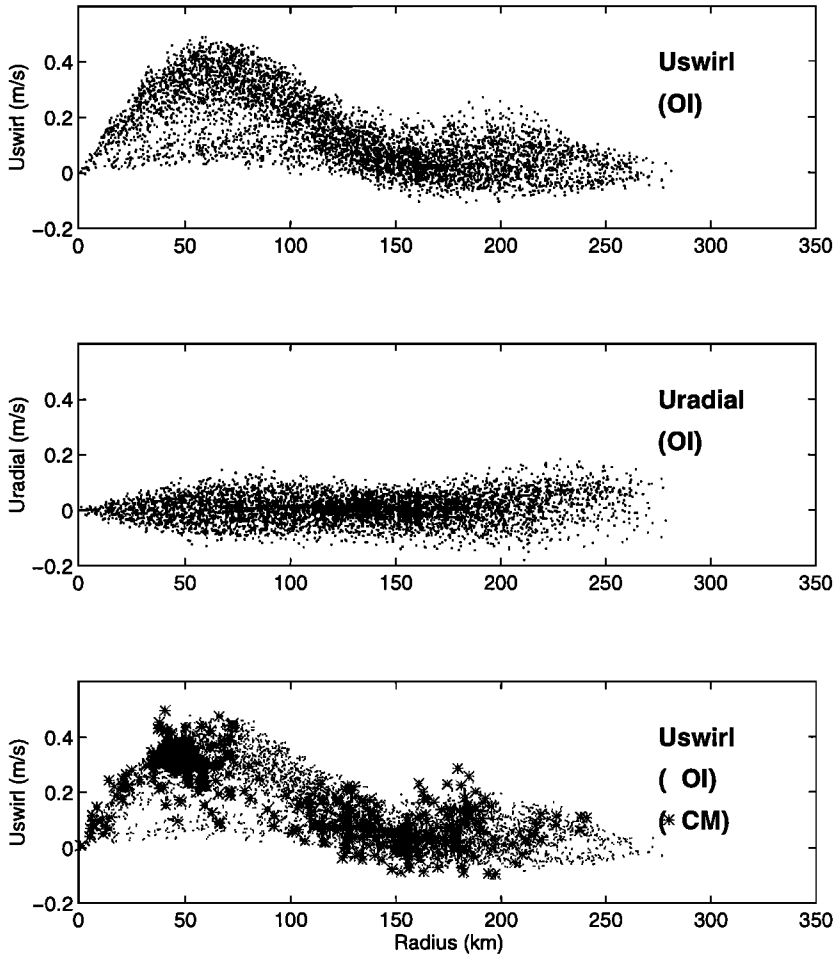

Figure 10. Scatter plot of 3500 m swirl and radial velocities (m s^{-1}) plotted as a function of distance to cyclone center. Positive values are counterclockwise and outward from center, respectively. (top) Optimally interpolated swirl velocities, (middle) optimally interpolated radial velocities, and (bottom) measured swirl velocities (asterisks) superimposed on optimally interpolated swirl velocities (dots).

any particular event. The cyclones started their lives with essentially the same eddy radius (R_{eddy}, defined as the radius beyond which the average falls below background) and radius to maximum velocity ($R_{u_{max}}$) that they ended with. Second, the shape of u_{swirl} as a function of radius, $R_{u_{max}}$, and R_{eddy} were all strikingly similar from event to event. The maximum velocities achieved and the lifetimes of the cyclones varied from event to event, but the size and structure were remarkably consistent. These plots suggest that $R_{eddy} = 130$ km and $R_{u_{max}} = 55$ km. For comparison, the Rossby internal radius of deformation (L_R) was calculated for the deep ocean as $L_R = NH/f$, where $N = 10^{-3}$ s^{-1} (a typical subthermocline value for the Brunt-Vaisala frequency [*Pedlosky*, 1987]), $H = 3000$ m (the scale height of the deep ocean), and $f = 10^{-4}$ s^{-1} (the Coriolis parameter). This gives $L_R = 30$ km. A thermocline layer value for (L_R) can also be calculated, using $N = 5 \times 10^{-3}$ s^{-1} (a typical thermocline value for the Brunt-Vaisala frequency [*Pedlosky*, 1987]) and $H = 1000$ m (typical depth of upper ocean), giving $L_R = 50$ km. This may be the more important measure since the dynamics appear to be controlled by upper ocean processes [*Savidge and Bane*, this issue].

The shear and curvature relative vorticities were calculated from the average swirl velocities as a function of radius. Finite difference estimates of shear vorticity ($\zeta_{sh} = \partial u_{swirl}/\partial R$) were made between the centers of the radial bins and interpolated to bin centers. Curvature vorticity was calculated as $\zeta_{cv} = u_{swirl}/R$, where u_{swirl} is the average swirl velocity in a particular radial bin and R is the radius at the center of that bin. The estimates for event F (Figure 12) show positive curvature vorticity, decreasing from a maximum near 8×10^{-6} s^{-1} at small radii to near zero values at radii greater than R_{eddy}. Shear vorticity is positive at radii $< R_{u_{max}}$, decreasing from a maximum of about 6×10^{-6} s^{-1} at small radii to near zero at $< R_{u_{max}}$ to about -5×10^{-6} s^{-1} values somewhere between $R_{u_{max}}$ and R_{eddy}. The total relative vorticity is positive at radii $< R_{u_{max}}$, decreasing from a maximum of about 15×10^{-6} s^{-1} at small radii. Values at radii $R_{u_{max}} < R < R_{eddy}$ are approximately 25% of the maximum value, approaching zero at $R \geq R_{eddy}$. This indicates that water parcels located farther from cyclone center than $R_{u_{max}}$ have not had their relative vorticity modified substantially from that outside the cyclone during cyclone spin up. This is true even for a wa-

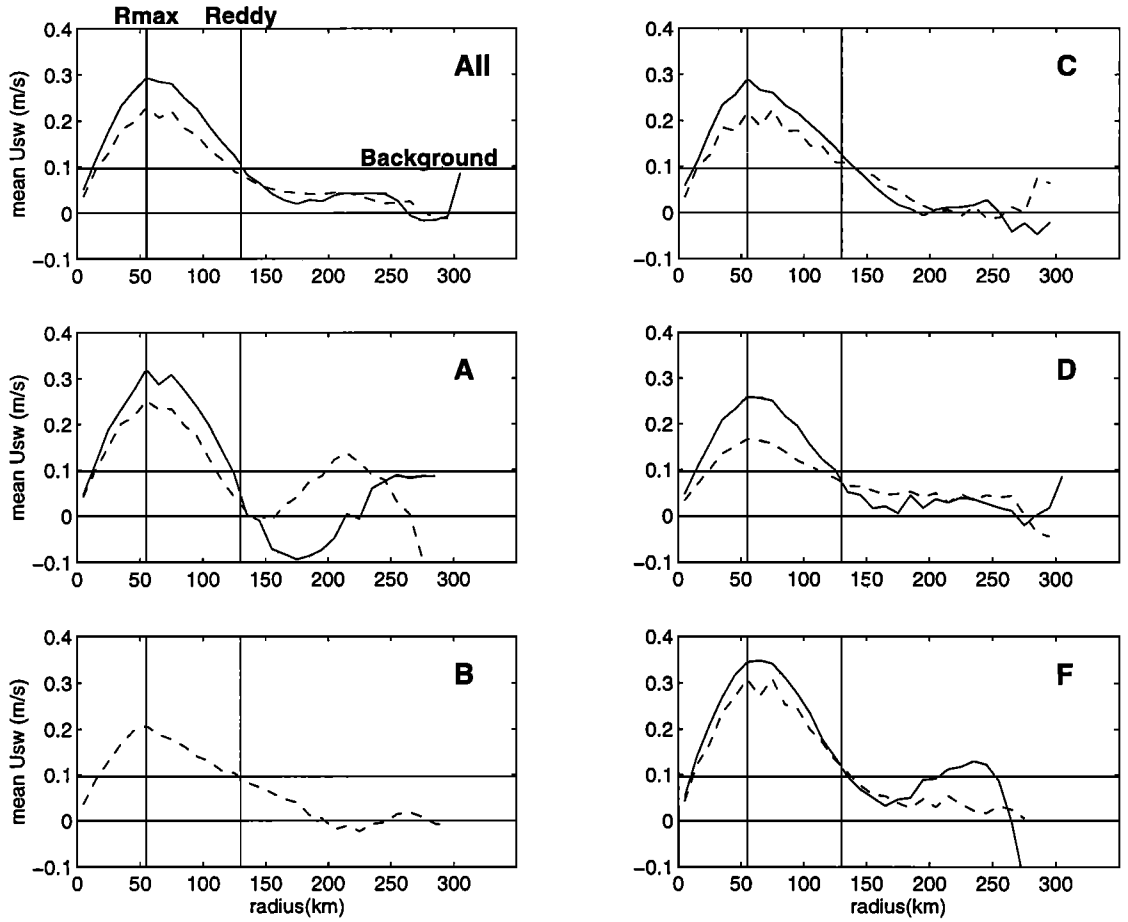

Figure 11. Average swirl velocity as a function of radius for each event and for all events pooled. Averages are taken over all azimuths, for developing days of the cyclones (dashed line) and fully developed days (solid line). R_{eddy} in these plots is the apparent radius beyond which the average velocity falls below background, 130km. $R_{u_{max}}$ is the apparent radius of maximum average velocity, 55km.

ter parcel that has been accelerated and is circulating in the cyclone with a substantial swirl velocity, since its positive curvature vorticity is nearly balanced by a negative shear vorticity (Figure 12, bottom 3 panels). Results from other events are consistent with these values.

6. Deep Cyclone Vertical Structure

The SYNOP moored current meter observations were rather sparse in the vertical, especially beneath the main Gulf Stream jet, where there was no instrumentation between 1000 and 3500 m depth. In this section, the vertical extent of the strong organized horizontal velocities seen at 3500 m is investigated, first by comparing velocities at the different measurement levels and then from estimating vertical shear using the thermal wind assumption.

If the cyclonic velocities observed at 3500 m existed at the upper three measurement levels, the total velocities measured in the upper ocean would be a sum of the relatively large Gulf Stream jet velocities plus the cyclone swirl velocities. Cyclonic velocities of the same order as those at 3500 m (up to 0.5 m s^{-1}) would be well masked at the jet levels by the strong Gulf Stream jet velocities (up to 2.5 m s^{-1}). To remove the jet signature, the measured velocities at all levels were adjusted by subtracting the Gulf Stream stream-coordinate average velocity of *Johns et al.* [1995]. The direction the Gulf Stream was flowing relative to a given mooring and the cross-stream location of a mooring on a given day were determined for the *Johns et al.* [1995] study, and that information has been utilized here. In addition, a correction for Gulf Stream curvature was also made, since by the gradient wind balance, the effect of positive (negative) curvature is to diminish (increase) the magnitude of streamwise velocity from its geostrophic value, given identical cross-stream pressure gradients. Estimates of Gulf Stream curvature in the vicinity of the moorings as a function of time were also calculated by *Johns et al.* [1995] and are utilized here to make this correction, the magnitude of which is quite small.

The "residual" velocities (the measured velocities minus the stream-coordinate average and the curvature correction) are shown for the four measurement levels 3500, 1000, 700, and 400 m, on one day during event C (Figure 13). Optimal interpolation was used to calculate pressure fields from the residual velocities such that the velocities and the pressure gradients are geostrophically balanced. These plots show cyclones at 3500, 1000, and 700 m. During periods when

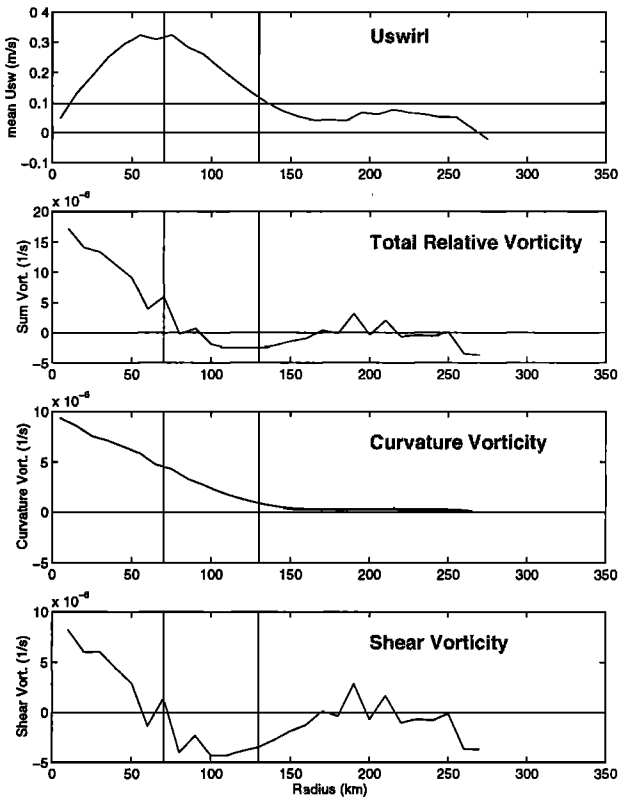

Figure 12. Mean velocity and relative vorticity as a function of radius for event F. Panels are, from top to bottom as labeled, average swirl velocity as a function of radius, total relative vorticity (curvature plus shear vorticity), curvature vorticity, and shear vorticity.

the cyclone was at its strongest at 3500 m, a cyclone was also evident at 400 m (such a day is not shown in the figure). Standard errors for these calculations were calculated as the square root of the sum of the squares of the standard errors from the mooring location time series [*Shay et al.*, 1995], and those from the stream coordinate means [*Johns et al.*, 1995], interpolated to mooring locations and rotated into the local downstream direction. Whether or not a cyclone was seen in the residual velocities at 400 m depends crucially on the magnitudes of the means in the cross-stream direction used to make the corrections from the measured velocities. The standard deviations of the *Johns et al.* [1995] cross-stream means are larger than the means themselves, so the cross-stream corrections were conditionally set to zero to investigate their contribution to the previous calculations. When that was done, the residual velocities showed a cyclone at 400 m throughout the events. Flows at 200 and 50 m (as measured by a few limited acoustic dopplar current profiler moorings) were found to be consistent with cyclones at those levels as well (not shown).

Next, the vertical extent of the strong organized cyclonic velocities observed at 3500 m were investigated using thermal wind velocity shear estimates. According to thermal wind balance, the small horizontal density gradients generally seen in the deep ocean would support only very small vertical shear in low Rossby number flows there. Using characteristic velocity and length scales for the cyclone events of 0.40 m s^{-1} and 55 km, respectively, a Rossby number of $R_o = U/fL \simeq 0.08$ was estimated for the latitude of the measurements, indicating that the cyclones were low Rossby number features. Thermal wind vertical shear was calculated at 3500 and 1000 m from horizontal density gradients there. These gradients were calculated from measured temperatures as described in section 2. Typical values of vertical shear at 3500 m in this location were $\sim 5 \times 10^{-5}$ s^{-1}. If those values held over, say, 1000 m depth in the deep ocean, the large velocities seen at 3500 m would change by only 0.05 m s^{-1} over that depth. Values of vertical shear at 1000 m range from $\sim 5 \times 10^{-5}$ to $\sim 5 \times 10^{-4}$ s^{-1}.

To assess the vertical extent over which the low shear estimates at 3500 m held, the thermal wind vertical shear estimates were plotted as a function of thermocline depth, taken to be the depth of the Z12 surface, here bilinearly interpolated from the grid points to mooring locations. In Figure 14, only the $\partial u/\partial z$ component of vertical shear for event F has been shown (u is velocity from left to right in the Central Array). The results discussed below are essentially identical for the $\partial v/\partial z$ component and for all other events. Vertical shear estimates at 3500 m are not a strong function of the thermocline depth, while estimates at 1000 m are (Figure 14, top). This suggests that the vertical variation of vertical shear was quite small from the 3500 m level up through the water column until the base of the thermocline was encountered, at which point the vertical shear increased, reaching values an order of magnitude larger than those in the subthermocline water. The large vertical shear values near the thermocline are associated with the large vertical shear in the Gulf Stream jet. Finite difference estimates of average vertical shear between 3500 and 1000 m can be made from the measured velocities at those levels. These estimates, also plotted as a function of thermocline depth (Figure 14, bottom), are similar in magnitude to the thermal wind estimates at 3500 m, suggesting that over the water column between 3500 and 1000 m, the lower level values dominate. This implies that the strong cyclones seen at 3500 m extend throughout much of the lower water column. The residual velocity calculations described above further suggested that the cyclones extended up through the thermocline. The dynamical analysis associated with this descriptive work [*Savidge and Bane*, this issue] is consistent with this, as it indicates that the cyclones extend to the ocean surface.

7. Cyclone Coherence and Water Parcel Trajectories

It is tempting to consider the cyclones described thus far as coherent structures: as columns of water spinning and migrating relative to the bathymetry and the thermocline topography. To assess how coherent the cyclonic flow features were, water parcel trajectory studies were undertaken to determine if the water parcels followed the cyclones. The OI horizontal velocities at 3500 m were used to calculate trajectories of parcels starting within 70 km of the cyclone centers. A multidimensional fourth-order to fifth-order Runge-Kutta

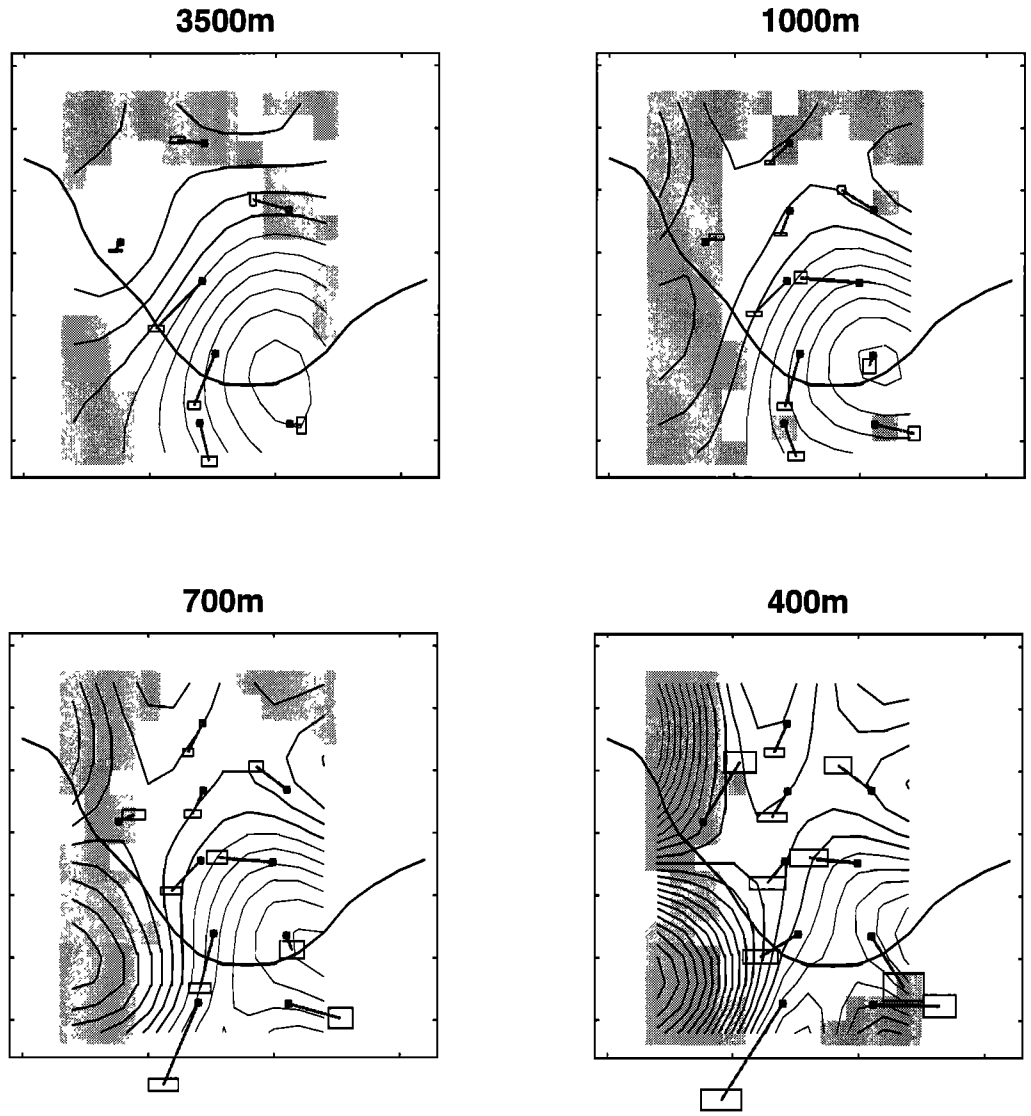

Figure 13. Horizontal maps of residual velocities with standard errors (vectors with boxes) and associated pressure fields assuming geostrophy, calculated from the residual velocities at each depth using OI (bold lines are positive pressure perturbations). Data shown are from May 15, 1989, a day during event C. The single boldest line is the 400 m contour of the depth of the 12°C isothermal surface, indicating the approximate path of the Gulf Stream jet. The pressure field contour interval is 2.5 x 10^2 Pa (0.025 dbar). The four panels are for the 3500, 1000, 700, and 400 m level, as labeled.

routine similar to that described by *Press et al.* [1992] was used to integrate the velocities in time and space. The velocities at a given time were first linearly interpolated from the nearest two time steps in the data set and then bilinearly interpolated in space from the grid locations.

This parcel tracking in a horizontal plane assumes that either the parcels stay at the depth at which they start or that the horizontal velocities at depths to which the parcels are likely to stray are quite similar to those at 3500 m. Assuming a linear vertical profile of vertical velocities between those at 700 m (calculated using the methods of *Lindstrom et al.* [1997]) and vanishing vertical velocities at the ocean bottom, vertical velocities at 3500 m during cyclogenesis are about $\pm 1 \times 10^{-3}$ m s^{-1} (about ± 100 m d^{-1}) over most of the region occupied by the cyclones. Therefore parcels can be expected to stay within 1000 m of 3500 m over 10 days or more. As seen in section 6, horizontal velocities should change very little over even twice that depth range, since the small vertical shear calculated for 3500 m appear to hold over much of the water column below the thermocline. This indicates that the parcel tracking discussed below should be valid over timescales of 10-20 days.

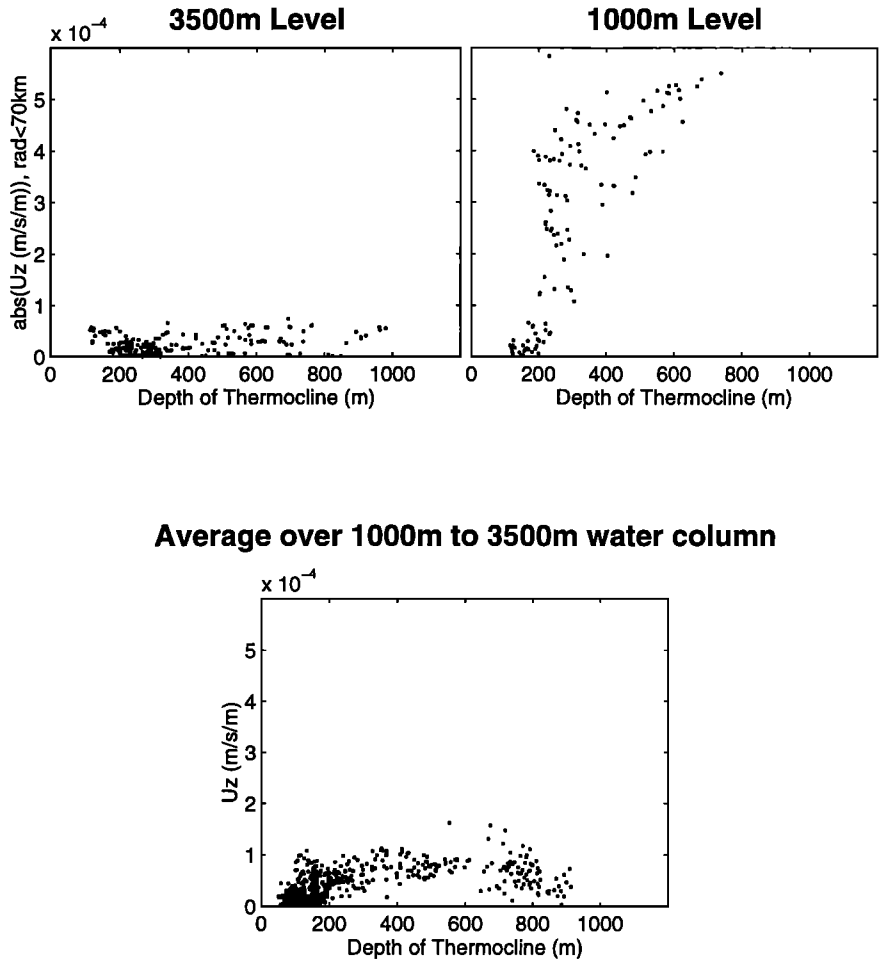

Figure 14. Vertical shear estimates ($\frac{\partial u}{\partial z}$ component) as function of thermocline depth for Event F. (top) Thermal wind estimates from data at the 3500 and 1000 m measurement levels, as indicated. (bottom) Average shear over the 1000-3500 m water layer from measured velocities at 1000 and 3500 m depth, calculated as $\Delta u/\Delta z = (u_{1000\ m} - u_{3500\ m})/2500\ m$.

Parcel tracks relative to cyclone center for several parcels seeded on two different days in event F show differing behavior (Figure 15). The parcels seeded on event day 0 do not remain with the cyclone, while those seeded on event day 12 stay with the cyclone. Parcels seeded on other days (not shown) indicate that after about event day 9 parcels consistently stay with the cyclone. The development of the deep cyclone over this time period is illustrated in Figure 2. The track of the low pressure feature over this time period is shown in Figure 6. This allows us, to some extent, to consider the cyclones as coherent bodies of water when assessing their dynamics in terms of conservation of material and dynamical properties. The same conclusion holds for event C (not shown). Conversely, the loss of parcels from the cyclone vicinity during the first several days of events C and F suggests that the cyclones are not coherent bodies of water over their first several days and that the appealing concept of a coherent column of water stretching as it travels over deepening topography is inappropriate here, since a coherent column of water does not follow the migrating low pressure centers.

Another interesting feature illustrated by the parcel tracks is that over the lifetime of an event, 6-9 weeks, the parcels travel only a few times around the cyclone center. This is consistent with the average velocity versus radius plots seen previously. For example, for an average maximum velocity of 0.20 m s^{-1} at 55 km radius, the time required to travel the circumference would be 20 days. This fact is helpful in visualizing the spun-up cyclones as a slow, relatively steady rotation of the water column over an extended period of time.

8. Discussion and Summary

Strong coupling between the Gulf Stream and the underlying water column results in the spin-up of strong cyclones in the deep flow (swirl speeds up to 0.5 m s^{-1} at 3500 m) that develop in response to the growth of large amplitude meander troughs in the path of the Gulf Stream jet. The large amplitude troughs and deep cyclones develop rapidly, over 10-20 days, and persist for periods of 6-9 weeks. Typically, a small amplitude Gulf Stream meander "stalls" near 68°W and begins to amplify, perhaps triggered by ring-Stream in-

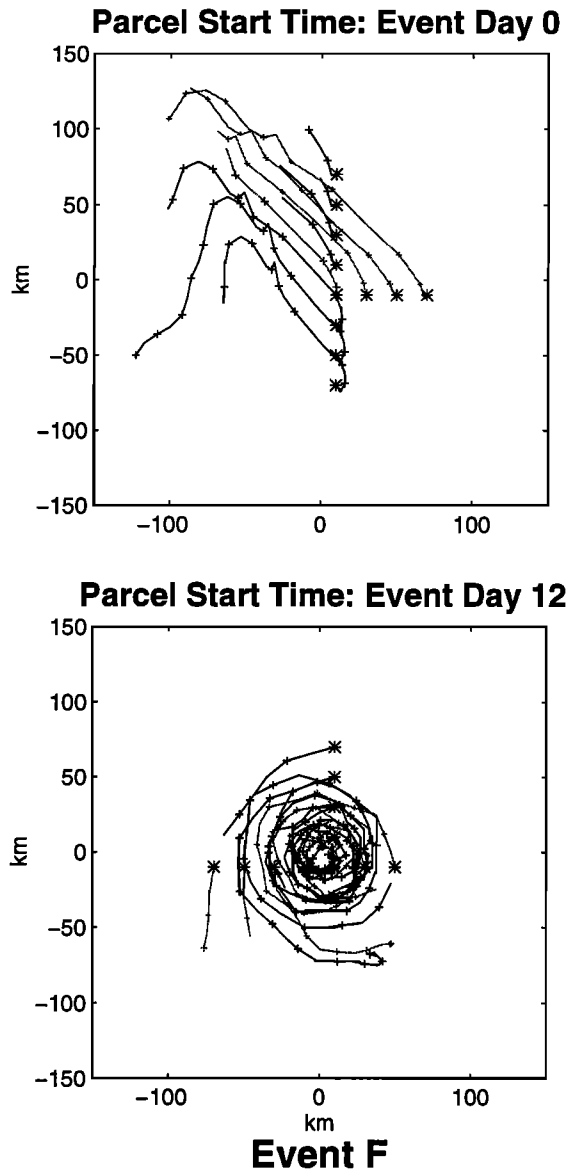

Figure 15. Parcel trajectories at 3500 m depth relative to cyclone center for parcels seeded on two different days during event F. Starting locations (asterisks) and daily noon positions of parcels (crosses)are indicated. Parcels were tracked either for 20 days or until they left the array. (top) Starting day 0, (bottom) starting day 12.

teractions immediately downstream. Thus far, only circumstantial evidence supports the importance of ring-Stream interactions, in that such interactions were apparent in satellite imagery in all of the observed cases of deep cyclogenesis during SYNOP. As the amplitude of troughs in the Gulf Stream jet increases, the currents at 3500 m strengthen and turn, forming a cyclonic circulation pattern. During SYNOP, six well-defined instances of meander trough amplification and deep cyclogenesis occurred, constituting 35% of the time.

The structure of the cyclones at 3500 m is characterized by increasing velocity from the cyclone center out to some radius of maximum velocity and decreasing velocity beyond that radius. This structure is apparently robust. Cyclone radius and the radius to maximum velocity are consistently about 130 and 55 km, respectively, changing very little over the lifetime of an event or from event to event. Evidence of cyclones at upper measurement levels and the low vertical shear values apparent in the deep water below the thermocline indicate that the cyclones extend through much of the water column; from the benthic boundary layer up into and possibly above the thermocline. Further investigation discussed by *Savidge and Bane* [this issue] supports the existence of cyclones through the entire water column.

While the two strongest events were characterized by migration of the low pressure center over steeply deepening bathymetry during the early days of their lifetimes, it does not appear that simple column stretching of the water below the thermocline resulted, since at the same time the cyclone columns moved with respect to the Gulf Stream jet axis and the offshore deepening of the thermocline. Individual water parcels did not stay with the cyclones during this early migration. When the cyclones became more stationary, individual water parcels did remain with the cyclones.

Acknowledgments. Much of this work stands on the shoulders of the work of Randy Watts and his group at the Graduate School of Oceanography of the University of Rhode Island. Thanks to Randy, Xiaoshu Qian, Karen Tracey, and Stephan Howden for their input and assistance. Thanks also to Thomas Shay here at UNC-CH for his help and insight. The collection of the SYNOP data was supported by NSF grant OCE-8717141 and by ONR grant N00014-87-K-0233 to the University of North Carolina at Chapel Hill. This analysis of the SYNOP data was supported by NSF grant OCE-9302816 and by ONR grant N00014-92-J-1683 to John Bane at the University of North Carolina at Chapel Hill, by ONR AASERT grant N00014-93-1-1012, and by the Marine Sciences Program at the University of North Carolina at Chapel Hill.

References

Armi, L., and N. A. Bray, A standard analytic curve of potential temperature versus salinity for the western North Atlantic, *J. Phys. Oceanogr., 12*, 384–387, 1982.

Bower, A. S., and N. G. Hogg, The structure of the Gulf Stream and its recirculations at 55°W, *J. Phys. Oceanogr., 26*, 1002–1022, 1996.

Bretherton, F. P., R. E. Davis, and C. B. Fandry, A technique for objective analysis and design of oceanographic experiments applied to MODE-73, *Deep Sea Res., 23*, 559–582, 1976.

Cronin, M., Eddy-mean flow interaction in the Gulf Stream at 68°W, Ph.D. thesis, Univ. of R. I., Kingston, 1993.

Cronin, M., and D. R. Watts, Eddy-mean flow interaction in the Gulf Stream at 68°W: Part 1. Eddy energetics, *J. Phys. Oceanogr., 26*, 2107–2131, 1996.

Csanady, G. T., Radiation of topographic waves from Gulf Stream meanders, *Cont. Shelf Res., 8*, 673–686, 1988.

Hendry, R., On the structure of the deep Gulf Stream, *J. Mar. Res., 40*, 119–142, 1982.

Hogg, N. G., Topographic waves along 70°W on the continental rise, *J. Mar. Res., 39*, 627–649, 1981.

Hogg, N. G., Mooring motion corrections revisited, *J. Atmos. Oceanic Technol., 8*, 289–295, 1991.

Holton, J. R., *An Introduction to Dynamic Meteorology*, second ed., 391 pp., Academic, San Diego, Calif., 1979.

Howden, S. D., Processes associated with steep meander development in the Gulf Stream near 68°W, Ph.D. thesis, 229 pp., Univ. of R. I., Kingston, 1996.

Johns, W., and D. R. Watts, Time scales and structure of topographic Rossby waves and meanders in the deep Gulf Stream, *J. Mar. Res.*, *44*, 267–290, 1986.

Johns, W. E., T. J. Shay, J. M. Bane, and D. R. Watts, Gulf Stream structure, transport, and recirculation near 68°W, *J. Geophys. Res.*, *100*, 817–838, 1995.

Kelley, E. A., G. L. Weatherly, and J. C. Evans, Correlation between surface Gulf Stream and bottom flow near 5000 meters depth, *J. Phys. Oceanogr.*, *12*, 1150–1153, 1982.

Kim, H.-S., and D. R. Watts, An observational streamfunction in the Gulf Stream, *J. Phys. Oceanogr.*, *24(12)*, 2639–2657, 1994.

Lee, T., and P. Cornillon, Propagation and growth of Gulf Stream meanders between 75°and 45°W, *J. Phys. Oceanogr.*, *26*, 225–241, 1996.

Lindstrom, S., X. Qian, and D. R. Watts, Vertical motion in the Gulf Stream and its relation to meanders, *J. Geophys. Res.*, *102*, 8485–8503, 1997.

Luyten, J. R., Scales of motion in the deep Gulf Stream and across the continental rise, *J. Mar. Res.*, *35*, 49–74, 1977.

Palmen, E., and C. W. Newton, *Atmospheric Circulation Systems*, first ed., 603 pp., Academic, San Diego, Calif., 1969.

Pedlosky, J., *Geophysical Fluid Dynamics*, 2nd ed., 710 pp., Springer-Verlag, New York, 1987.

Pickart, R., Gulf Stream generated topographic Rossby waves, *J. Phys. Oceanogr.*, *25*, 574–586, 1995.

Press, W. H., S. A. Teukolsky, W. T. Vetterling, and B. P. Flannery, *Numerical Recipes in FORTRAN*, 2nd ed., 963 pp., Cambridge Univ. Press, New York, 1992.

Qian, X., and D. R. Watts, The SYNOP experiment: Bottom pressure maps for the Central Array, May 1988 to August 1990., *Tech. Rep. 92-3*, Univ. of R. I., Kingston, 1992.

Savidge, D. K., Cyclogenesis in the deep Atlantic associated with Gulf Stream trough formation, Ph.D. thesis, Univ. of N. C., Chapel Hill, 1997.

Savidge, D. K., and J. M. Bane, Cyclogenesis in the deep ocean beneath the Gulf Stream 2. Dynamics, *J. Geophys. Res.*, this issue.

Shay, T. J., J. M. Bane, D. R. Watts, and K. L. Tracey, Gulf Stream flow field and events near 68°W, *J. Geophys. Res.*, *100*, 22,565–22,589, 1995.

Thompson, J. D., and W. J. Schmitz, A limited-area model of the Gulf Stream: Design, initial experiments, and model-data intercomparison, *J. Phys. Oceanogr.*, *19*, 791–814, 1989.

Tracey, K. L., and D. R. Watts, The SYNOP experiment: Thermocline depth maps for the Central Array, October 1987 to August 1990., *Tech. Rep. 91-5*, Univ. of R. I., Kingston, 1991.

Watts, D. R., K. L. Tracey, J. M. Bane, and T. J. Shay, Gulf Stream path and thermocline structure near 74°W and 68°W, *J. Geophys. Res.*, *100*, 18,291–18,312, 1995.

J. M. Bane Jr. and D. K. Savidge, Department of Marine Sciences, University of North Carolina at Chapel Hill, CB# 3300 Venable Hall, Chapel Hill, NC, 27599. (dana@marine.unc.edu)

(Received December 18, 1997; revised November 20, 1998; accepted December 9, 1998.)